Numerical and experimental investigation of mixed-mode fracture of cement paste and interface under three-point bending test

ABSTRACT This paper shows 2D simulations of crack propagation in mode I and mixed mode (I and II) in a cementitious material at the material scale (known as local scale). There are two types of three-point bending tests modeled: eccentric loading on pre-notched cement paste samples and centered loading on three configurations of composite samples (cement paste linked to siliceous aggregate). These simulations, which were based on Cohesive Zone Models, were effective in forecasting fracture propagation and damage progression at the local scale.

Keywords Cement paste, Interface, Cohesive Zone Model, Fracture, Three-point flexural test bending.

I. INTRODUCTION

Concrete is a quasi- brittle material with a high degree of heterogeneity. It is a nearly brittle material with a high degree of variability. The presence of multiple phases in concrete (cement paste, sand, gravel, porosity, etc.) leads in a gradient of mechanical characteristics, notably around the aggregates, where an Interfacial Transition Zone (denoted ITZ) is formed. This disparity in microstructure characteristics has a significant impact on the process of damage and cracking, making fracture propagation in concrete difficult to predict.

The experimental results reveal that cracks can occur at the interfaces of relatively heterogeneous materials like concrete due to debonding and subsequently spread through the matrix, or vice versa. These observations highlight the significance of conducting a local numerical investigation of crack propagation at the level of pure cement paste and at the interface between the cement paste and the aggregate. Analyzing the phenomena of local crack propagation, two mechanisms are commonly distinguished: the emergence of a damaged zone at the crack tip and the occurrence of the crack. These mechanisms result in two numerical behaviors: (i) linear in the absence of cracking in the material; and (ii) nonlinear, related to the appearance of microcracks and damage or steady growth of cracks. The Cohesive Zones Model (CMZ) is one of the modeling methodologies used here for fracture mechanisms in heterogeneous materials. This model allows us to define the fracture as a displacement jump between cohesive elements. These numerical results will be compared to experimental results obtained through an experimental program described below.

II. SPECIMEN PREPARATION AND EXPERIMENTAL SET- UP

A. Samples

The studies in this paper are performed on two types of parallelepiped samples (dimensions: 10x10x30 mm^3) a specimen of cement paste notched at a 60° angle, and a composite made of cement paste attached to a silica-type aggregate (quartz) whose interface angle ranges between 30° and 90°(see Figure 1). The notch on the cement paste sample allows for the location of the crack's initiation. On composite specimens, a notch is not required because the contact with the aggregate is sufficient to locate the fracture (interfacial failure).

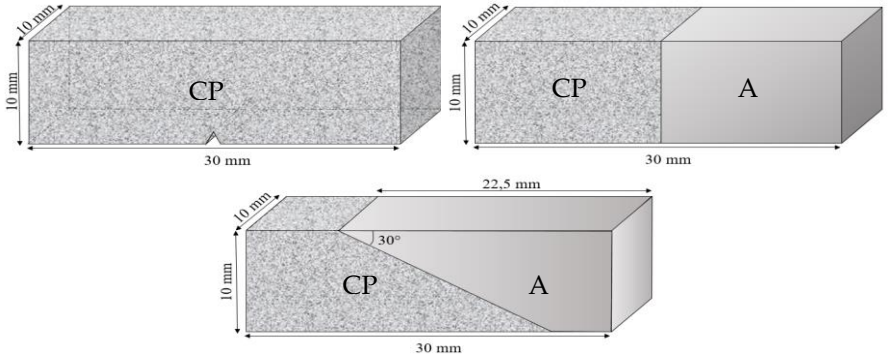

FIGURE 1. Specimens' geometries descriptions: cement paste (top left); straight aggregate composite with a 90° interface angle (top right); and 30° inclined aggregate composite (CP: Cement Paste and A: Aggregate).

The materials used to create the test specimens are listed in Tables 1 and 2. Silicone molds are used to make these specimens. After preparation, the samples are removed from the molds after 24 hours and conditioned in lime-saturated water for 40 days before being tested.

TABLE 1. Material properties.

Aggregate Mineralogical nature	Quartz (98% SiO_2)
Cement Paste Cement class Water-to-Cement ratio	 CEM I 52,5 R CE CP2 NF 0,47

TABLE 2. Cement's mineralogical and chemical compositions.

Components	C_3A	C_4AF	C_2S	C_3S
Content (%)	11	8	66	10

B. Experimental set-up

Concrete behavior at the local scale necessitates investigation under complex loading conditions. To answer this need, an adaptable three-point bending test bench (see Figure 2) was designed to allow for adjustment in loading conditions and specimen geometries.

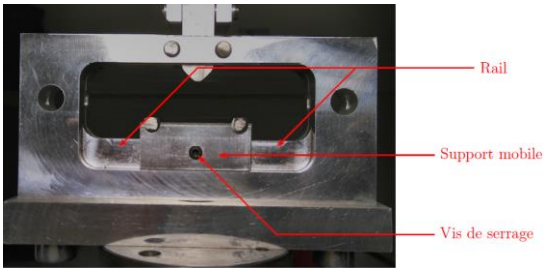

FIGURE 2. **Design of the modular three-point flexion bench [3].**

The distance between the point of load application and the center of the sample is referred to as the eccentricity dx in the following. For notched cement paste specimens, four loading positions with dx equal to 0 cm (centered loading), 2.5, 5, and 7.5 mm are tested experimentally. The composite specimens are tested on the same bending bench with centered loading (dx = 0), but with a difference in specimen configuration: in the first configuration (denoted C1), the loading is applied to the silica aggregate and, in the second (denoted C2), it is applied to the cement paste (see Figure 3).

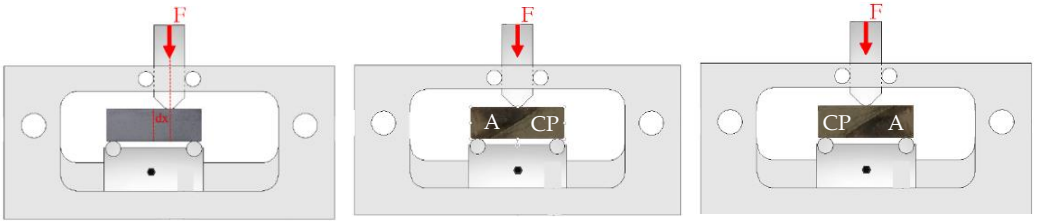

Cement Paste **C_1 - Composite** **C_2 - Composite**

FIGURE 3. Geometry and boundary conditioned of samples subjected to three-point bending test **(CP: Cement Paste and A: Aggregate).**

The specimen is positioned on the bending bench with the patterned side facing a high-resolution camera "acA5472-17um - Basler ace" mounted on a fixed gantry. Through precision control of the "MTS" compression machine, a loading speed of 10 μm/s is applied. After post-processing the findings with CIN digital image correlation software, the displacement field can be experimentally seen, from which the fracture propagation path within the specimens can be determined in both cases. The experimental results will be compared to the numerical results reported in the following sections.

III. MODELING

A. Numerical Model: Cohesive Zone Model - CZM

The Volumic-Cohesive Finite Elements (EFVC) approach involves "collapsing" the finite element mesh and considering the decohesion of the interfaces of its volumic elements. A so-called "cohesive" law links the finite components trying to describe the traction separation phenomena of the interface. In general, these cohesive laws connect the stress on the height of the crack lips to its displacement discontinuity. The cohesive zone at the interface is represented by

two damageable "springs" with two stiffnesses (denoted C_N and C_T), allowing the description of two failure modes: normal and tangential (see Figure 4).

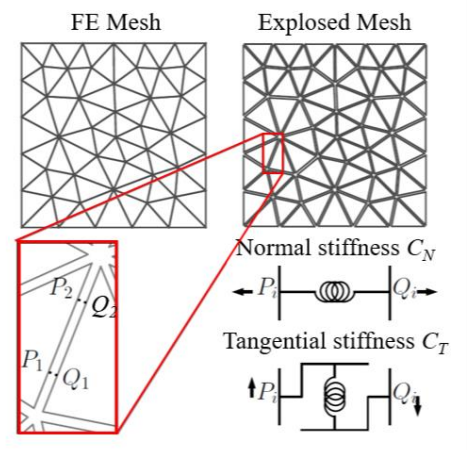

FIGURE 4. **Illustration of the concept of the Volumic-Cohesive Finite Element Approach [5].**

The "XPER" software [6, 7] developed at IRSN within the framework of the joint MIST laboratory (joint laboratory IRSN/CNRS/University of Montpellier) is the numerical tool employed.

For numerical simulations of cementitious materials, the cohesive law, known as MAL in XPER, was used [6, 7]. This cohesive law is determined by three parameters: σi (critical cohesive stress), w_i (cohesive energy), and C_i (initial cohesive stiffness) for each normal mode (i=1) and tangent mode (i=2) (see Figure 5).

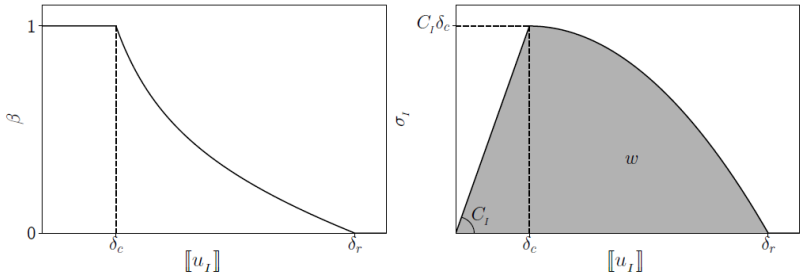

FIGURE 5. **The form of cohesive law applied. On the left: evolution of the damage according to the normal/tangent displacement discontinuity. On the right: cohesive stress associated with a normal/tangent displacement jump [5].**

A damage occurs between the elements after a critical displacement (δ_c) ($[\![u]\!] > \delta_c$) jump, regardless of the loading mixity (the same one in normal and tangent modes). Furthermore, the critical cohesive stresses of the normal and tangential modes may be given by the equation:

$$\sigma_N^{max} = C_N\,\delta_C = \left(\frac{1}{2} + \frac{C_N}{2C_T}\right)\sigma^{max} \quad \textbf{(1)}$$

$$\sigma_T^{max} = C_T\,\delta_C = \left(\frac{1}{2} + \frac{C_T}{2C_N}\right)\sigma^{max} \quad \textbf{(2)}$$

And the cohesive fracture energy by:

$$\omega_N = \left(\frac{1}{2} + \frac{C_N}{2C_T}\right)\omega \quad (3) \qquad \omega_T = \left(\frac{1}{2} + \frac{C_T}{2C_N}\right)\omega \quad (4)$$

It is important to note that the ratios of the normal and tangential cohesive stresses, as well as the cohesive energies, are identical.

B. Finite element meshes

For the two specimens, a uniform mesh of the Delaunay type with a characteristic size l_{mesh}=0.2 mm (see Figure 6) is generated in GMSH. Based on the calculations conducted during Delaume's thesis [2], a time step of 10^{-8} s is retained for the simulations. The vertical loading is delivered at a speed of 10 µm/s [5]. A volumic law is adopted between all the mesh's elements. Thus, a cohesive zone law is described for all interfaces: cement paste/cement paste, cement paste/aggregate and aggregate/aggregate.

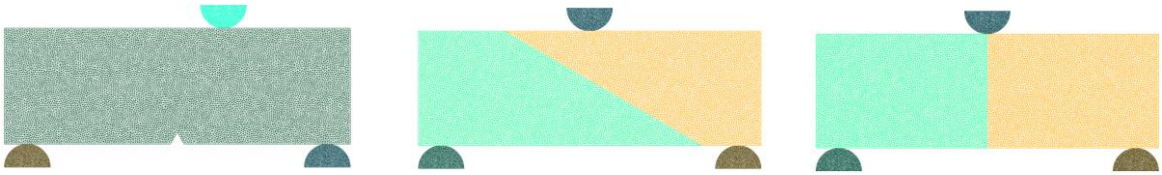

FIGURE 6. **The cement paste mesh for the eccentric three-point bending test is shown on the left. Composite mesh for the centered three-point bending test with aggregate slanted at 30° in the center. Composite mesh with straight aggregate (90°) on the right.**

The initial cohesive stiffness C_N and C_T for the three-point bending test on the notched cement pastes were determined using Blal's practical criterion [1] to limit the dependency of mechanical response (force/displacement) on the characteristic size of the mesh. The cohesive parameters for different phases are shown in Table 3. A ratio of 10 between normal and tangential values is proposed [8].

Table 3. **The elastic and cohesive properties of the different materials in use.**

	C_N [MPa/m]	**C_T [MPa/m]**	**σ_N [MPa]**	**σ_T [MPa]**	**w_N [J/m²]**	**w_T [J/m²]**	**E [MPa]**	**υ**
Cement paste	7.7×10^{11}	9.8×10^{11}	3.1	31	25	250	15×10^3	0.2
Interface	6.7×10^{11}	$8{,}8 \times 10^{11}$	0.4	3.1	2.5	25	-	-
Aggregate	1.21×10^{13}	5.1×10^{13}	6×10^2	6×10^3	10^5	10^6	65×10^3	0.2

C. Numerical results

Cement paste non-symmetrical three-point bending tests

First, the results of simulations performed on cement paste specimens with load eccentricities of 0, 2.5, 4, 5, 6, and 7.5mm are presented. Figure 7 shows a visualization of displacement fields.

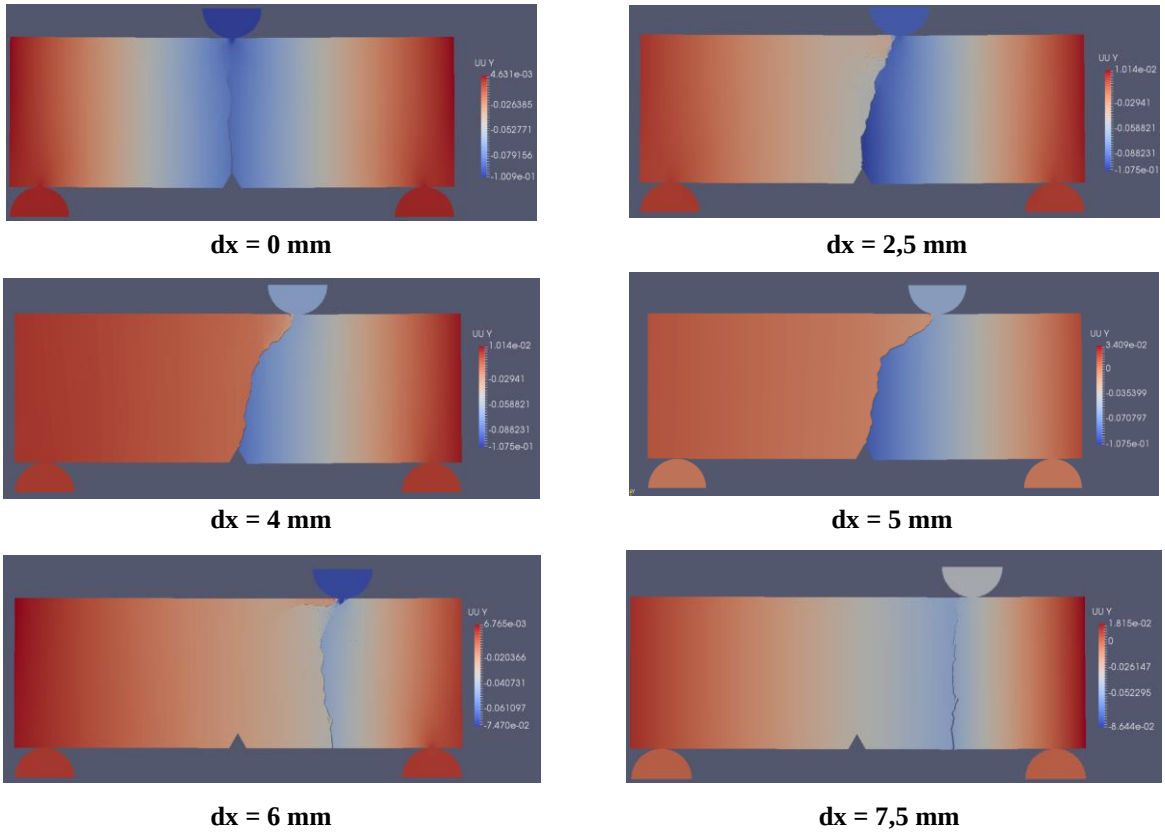

FIGURE 7. **Displacement fields of cement paste specimens in three-point flexural test with an eccentric load dx.**

In mode I, a crack propagates from the notch (concentrated load) throughout the center of the specimen when dx = 0 mm. The propagation is in mixed mode for dx = 2.5, 4 and 5 mm, and further fracture begins also in notch and reaches the place of application of the load. However, at an eccentricity of 2.5 mm, the crack first propagates in normal mode or mode I, then branched out in the cement paste to join the loading point application, which was not the case for dx = 4 and 5 mm, where the crack propagates in mixed mode from its initiation.

In the cases of eccentricity of 6mm and 7.5mm, however, the fracture does not initiate from the notch, but rather from the bottom edge of the specimen on the same horizontal side as the point load application.

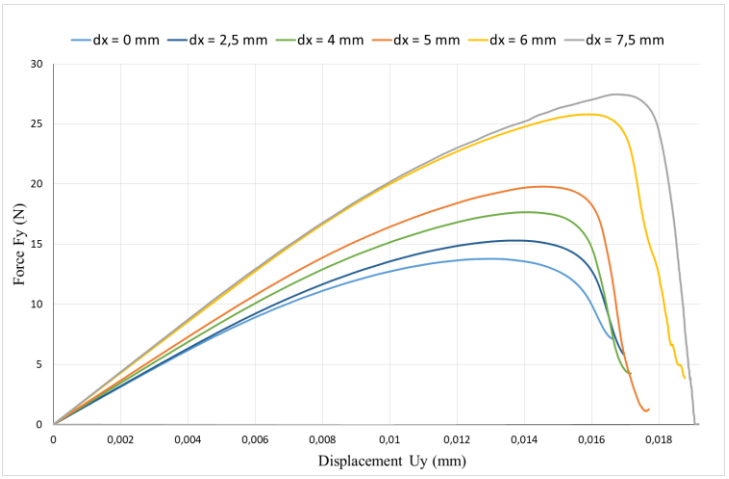

FIGURE 8. **Mechanical behaviors of cement paste specimens under non-symmetrical three-point bending tests (Fy : force applied vertically and Uy : displacement of the specimen in contact with the load application point).**

The curves in Figure 8 quantify these results. It is clear that the more the specimen is stressed in mixed mode, the stiffer the structure become, as does its resistance to rupture. Research by Y.S. Jenq [5] within the context of the investigation of the mixed pattern of crack propagation during a three-point bending on concrete prisms by displacing the notch regarding the centered loading supports our results.

Three-point bending tests with centered load on a composite with an oblique interface

Two composite specimen configurations, C1 and C2, are studied. For each configuration, three inclinations of the cement paste/aggregate interface (30°, 45°, and 60°) are considered in addition to a composite with a straight interface. Figure 9 represents the displacement fields and fracture propagation in these simulations.

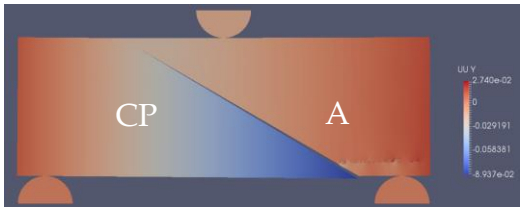

C_1 – 30°

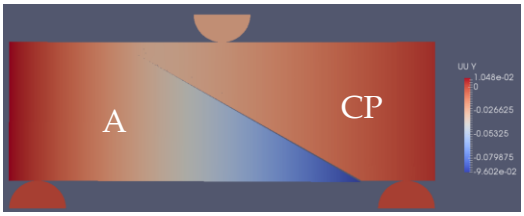

C_2 – 30°

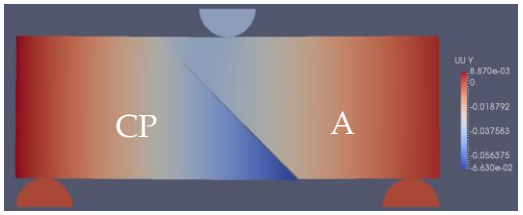

C_1 – 45°

C_2 – 45°

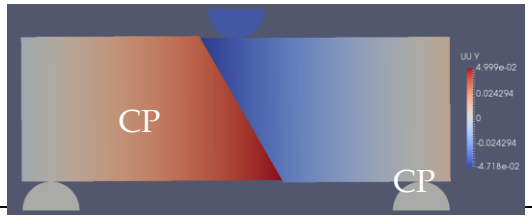

C_1 – 60°

C_2 – 60°

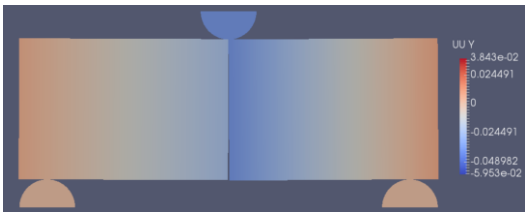

Straight – 90°

FIGURE 9. **Displacement fields of composite specimens subjected to three - point bending with centered load with inclined aggregate (30°, 45°, and 60°) and straight aggregate in two configurations (C1 and C2).**

The fracture propagates along the interface in both configurations C1 and C2 (the weakest phase). However, when the load is applied to the cement paste in the C2 configuration, the fracture spreading in the interface deviates in the cement paste towards the loading point.

The curves in Figure 10 indicate that as the interface is loaded in mixed mode by raising the inclination of the aggregate, the specimen's resistance and fracture energy increase. As a result, specimens from C1 configuration, where the load is applied to the silica aggregate, resist more than those from C2 configuration. This response is reasonably common due to the hardness of the contact point, as silica is more rigid than cement paste.

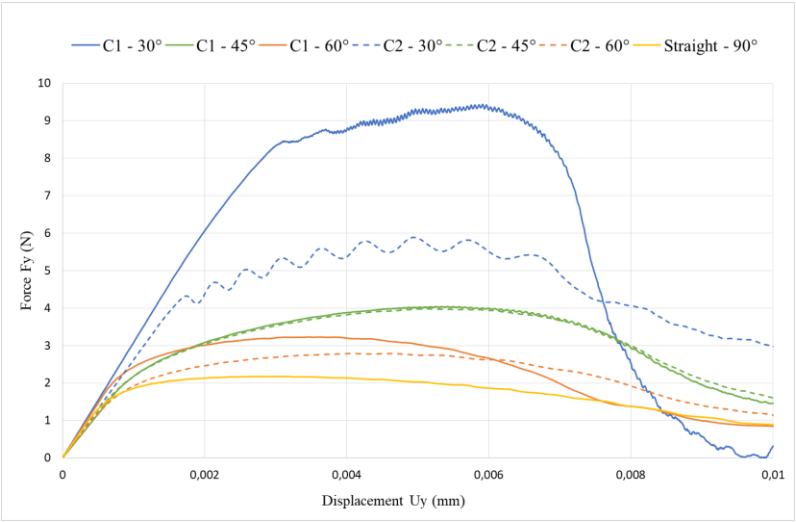

FIGURE 10. **Mechanical behaviors of composite specimens under symmetrical three-point bending tests (Fy : force applied vertically and Uy : displacement of the specimen in contact with the load application point).**

IV. COMPARISON BETWEEN EXPERIMENTAL AND NUMERICAL RESULTS

These tests were carried out experimentally on the two specimen types, due to the setup described in the preceding section. On notched cement paste specimens, four loading locations with eccentricities dx equal to 0 mm (centered loading); 2.5 mm; 5 mm; and 7.5 mm are investigated on 10 samples each. Three composite specimen forms are evaluated (6 samples per configuration) for the composite specimens: straight interface (90°); inclined interface at 30°; and

inclined interface at 60° where the loading is centered (dx = 0). Figures 11 and 12 show the experimental results of these tests, which are compared to a numerical simulation of a corresponding test.

The fracture propagates similarly experimentally and computationally in the eccentric three-point bending tests on cement paste (see Figure 11), where the fracture generally initiates at the notch and propagates in the cement paste in mode I when dx = 0 mm or in mixed mode in other circumstances.

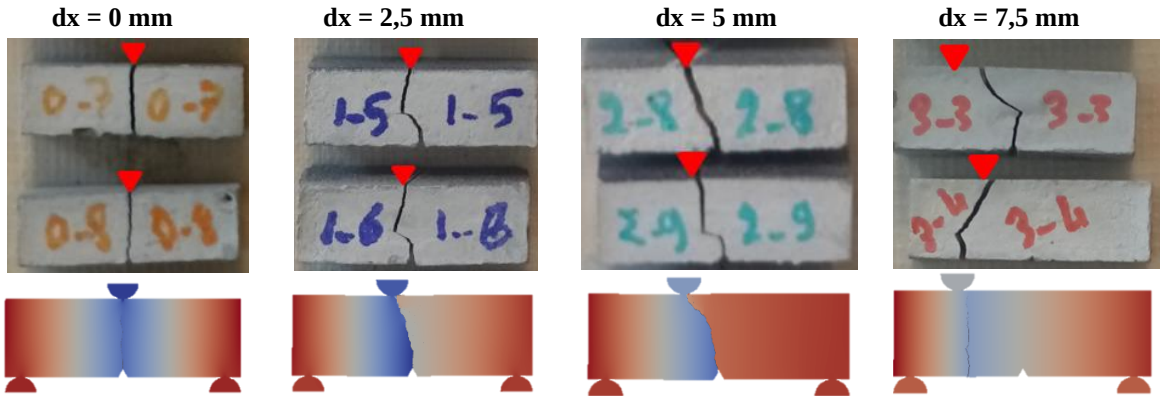

FIGURE 11. **Results of cement paste specimens under three points bending with an eccentric load of dx: Top, experimentally (rupture profiles); Bottom, numerically (rupture profiles and displacement fields).**

For the composite test results, the crack begins and propagates in the cement paste, then bifurcates to propagate in the interface in the C1 configuration. In the case of C2 configuration, the fracture propagates mostly in the interface and the cement paste after beginning on the tensile face at the matrix-aggregate connection.

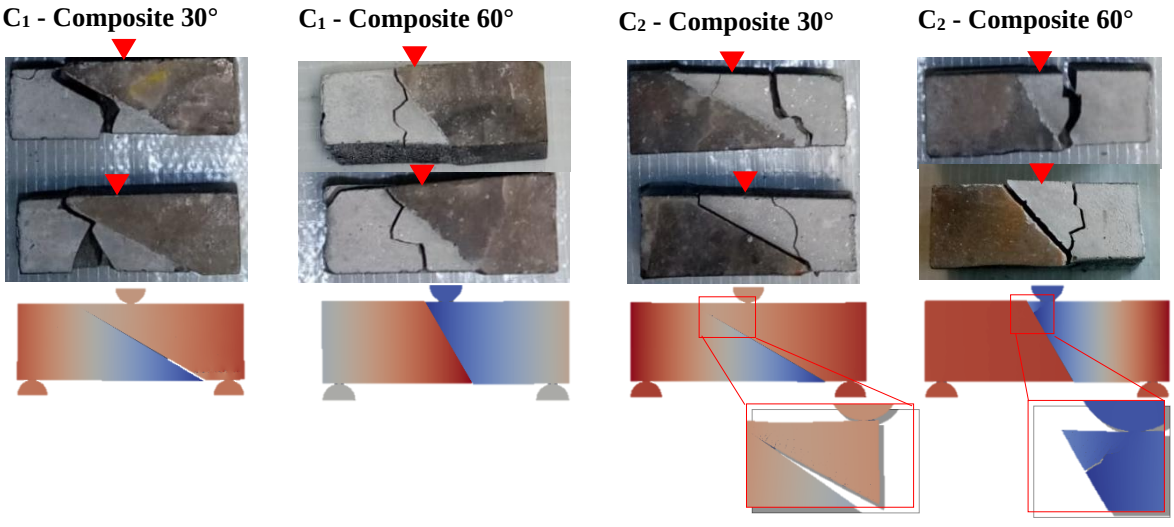

FIGURE 12. **Results of composite specimens under three points bending with a centered load: Top, experimentally (rupture profiles) and bottom, numerically (rupture profiles and displacement fields).**

This paper summarizes local-scale simulations of the mechanical behavior of cement paste and of the cement paste/aggregate interface under loading in normal mode and in mixed mode by a three-point bending device adapted for each specimen. The modeling of the cracking rests on the Models of Cohesive Zones. A cohesive law is introduced on all mesh interfaces.

The simulations match the present experimental results. Therefore, the numerical findings demonstrate that when the mixing ratio is high, the fracture energy and material resistance are significant for the two sample types: cement paste and composite. However, despite the similarity of experimental and numerical responses in terms of crack path, the experimental results do not match to those acquired numerically.

On the other hand, we find a brittle mechanical behavior of the cement paste and the interface of composite samples in which the fracture forms instantly and spreads swiftly. While a ductile behavior is numerically obtained, and the fracture propagation is smoother.

In the following steps, the experimental results will be compared to numerical simulations in order to calibrate and estimate the cohesive parameters of the numerical model.

VI. REFERENCES

[1] Blal, N., Daridon, L., Monerie, Y., & Pagano, S. (2013). Micromechanical-based criteria for the calibration of cohesive zone parameters. Journal of computational and applied mathematics, 246, 206-214.

[2] Delaume, E., Daridon, L., Dubois, F., Monerie, Y., & Perales, F. (2017, May). Méthode de raffinement local adaptatif multi-niveaux pour la fissuration des matériaux hétérogènes. In 13e colloque national en calcul des structures.

[3] Gîrboveanu, A. (2020). Approche multi-échelle de la dégradation chimique de matériaux cimentaires Application à la durabilité des ouvrages en béton (Doctoral dissertation, Université Montpellier).

[4] Jenq, Y. S., & Shah, S. P. (1988). Mixed-mode fracture of concrete. International Journal of Fracture, 38(2), 123-142.

[5] Lhonneur, J. (2021). Approche par changement d'échelle du vieillissement des bétons : expérimentations et simulations numériques (Doctoral dissertation, Montpellier).

[6] Perales, F., Bourgeois, S., Chrysochoos, A. and Monerie, Y. (2008). Two field multibody method for periodic homogenization in fracture mechanics of nonlinear heterogeneous materials. Engineering Fracture Mechanics, 75(11), pp.3378-3398.

[7] Perales, F., Dubois, F., Monerie, Y., Piar, B., & Stainier, L. (2010). A nonsmooth contact dynamics-based multi-domain solver : code coupling (xper) and application to fracture. European Journal of Computational Mechanics/Revue Européenne de Mécanique Numérique, 19(4), 389-417.

[8] Socie, A., Dubois, F., Monerie, Y., & Perales, F. (2021). Multibody approach for reactive transport modeling in discontinuous-heterogeneous porous media. Computational Geosciences, 25(5), 1473-1491.